



## BEHAVIOR OF MULTIPLE BROADBAND GROUND MOTION SIMULATION TECHNIQUES ON THE SCEC BROADBAND PLATFORM

Jeffrey R. BAYLESS<sup>1</sup>, Paul G. SOMERVILLE<sup>2</sup>, and Andreas A. SKARLATOUDIS<sup>3</sup>

The Southern California Earthquake Center (SCEC) Broadband Ground Motion Simulation Platform (BBP) is an important resource for researchers and practitioners who need to use strong ground motion simulations. The BBP allows a user (who need not be the developer of any simulation procedure) to generate ground motions for a particular earthquake scenario using physics-based simulation methods. The BBP provides the user with the flexibility to select from various alternative approaches for generating the earthquake rupture description, modelling low- and high-frequency wave propagation, and options for incorporating non-linear site effects. The end product of a BBP simulation is a set of three-component broadband synthetic seismograms at the desired station locations.

The BBP is part of the SCEC Community Modelling Environment in which SCEC scientists collaborate in the construction of shared data bases and computational platforms. While the BBP is under continuous ongoing development, the first validation phase of the BBP was recently evaluated by Dreger et al. (2013) for simulated pseudo-spectral acceleration (Sa) using version 13.6.1 of the BBP code. The Dreger et al. (2013) evaluation focused on the mean ground motion estimates for five simulation methods. The first part of the validation considered the bias of simulation results with respect to observations for seven validation events. In the second part, simulated Sa was compared with median predictions from published Ground Motion Prediction Equations (GMPEs). Based on the validation tests the EXSIM, G&P and SDSU methods were determined to be suitable for broadband simulation of median Sa from 0.01s to 3s period within the validation magnitude range (Dreger et al, 2013). The validated methods, their developers, and references are listed in Table 1.

Table 1. BBP Validated Methods

Method identifier	Developers (affiliations)	Key references (Latest published documentation)
EXSIM	Gail Atkinson, Karen Assatourians (UWO)	Motozedian and Atkinson (2005), Atkinson et al. (2009), and Boore (2009)
G&P: Graves and Pitarka	Robert Graves (USGS), Arben Pitarka (LLNL)	Graves and Pitarka (2010)
SDSU Method	Kim Olsen, Rumi Takedatsu (SDSU)	Mai et al. (2010), and Mena et al. (2010)

In the BBP validation project described above, as well as in previous validation projects (Bayless et al., 2011), comparisons were made for each technique between simulations and recordings, and between simulations and GMPEs. However, rigorous comparisons directly between the results of the different modelling techniques were not performed. In this study we evaluate how the simulation methods compare with each other given the same rupture scenarios. These insights will serve as a baseline for referencing the future differences observed between models; a) when default parameter

<sup>1</sup> Graduate Engineer, URS Corp, Los Angeles, jeff.bayless@urs.com

<sup>2</sup> Principal Seismologist, URS Corp, Los Angeles, paul.somerville@urs.com

<sup>3</sup> Seismologist, URS Corp, Los Angeles, andreas.skarlataoudis@urs.com

settings are adjusted in future sensitivity studies and, b) for earthquake validations and forward simulations, to allow for meaningful comparisons, including the ongoing Pacific Earthquake Engineering Research Center (PEER) NGA East validations and the South-western U.S. (SWUS) Ground Motion Characterization (GMC) SSHAC Level 3 study for the Diablo Canyon Power Plant (DCPP) and the Palo Verde Nuclear Generating Station (PVNGS).

The procedure we followed was to first develop a suite of five earthquake scenarios defined by location, moment magnitude, fault dimensions, geometry, mechanism, and hypocentre location. For each scenario, simulations were performed using all three simulation techniques, at 60 sites surrounding the fault in 20km and 50km rupture distance bands. Simulations were performed for rock site conditions at all sites. We calculate two primary comparison parameters over the ground motion period range 0.01-10.0s; Sa Ratio (Equation 1) and GMPE Ratio (Equation 2):

$$Sa\ Ratio(T, j, k) = \frac{1}{N} \sum_N^{i=1} \ln \left( \frac{RotD50(T)_{i,j}}{RotD50(T)_{i,k}} \right) \quad (1)$$

$$GMPE\ Ratio(T, j, k) = \frac{1}{N} \sum_N^{i=1} \ln \left( \frac{RotD50(T)_{i,j}}{RotD50(T)_{GMPE}} \right) \quad (2)$$

The Sa Ratio represents the natural logarithm of the ratio of RotD50 component (Boore, 2010). Sa at a given period (T) calculated from one simulation technique (j) relative to another (k), averaged over all recording stations (i, with N total stations). GMPE Ratio represents the natural logarithm of the ratio of simulated RotD50 to the GMPE prediction (the average of the PEER NGA GMPEs).

The results are presented as Ratio plots versus period showing the mean value over all sites, the 90% confidence interval (yellow band), and the mean plus or minus one standard deviation (green band). Sa Ratio and GMPE Ratio plots show the three simulation method combinations in separate rows. Finally, the maps of Sa Ratio and GMPE Ratio at each station were created to observe trends in the spatial behavior of the models. One map plot is created per spectral period; in each the left column is Sa Ratio, and the right column is GMPE Ratio.

All of these results are plotted for each earthquake scenario. Such a large number of figures cannot be included here, so we show example results in Figure 1 for EQ3.0; a Mw 6.6, 45° dipping reverse fault in southern California with depth to top of rupture equal to 3.0 km and a randomly specified hypocenter. Panel 1a shows the Sa Ratio plot, panel 1b shows the GMPE Ratio plot, panel 1c shows the Ratio maps for PGA, and panel 1d shows the Ratio maps for T=1.0s. It is important to note that the results presented are for a single realization of the EQ scenario, not using an average of multiple rupture realizations, as was done for the recent validation project (Dreger et al., 2013).

A good place to start the analysis is with the GMPE Ratios (Figure 1b). This is a primary test to see which methods are performing well, if the GMPE predictions are taken as “ground truth.” For EQ3.0 the simulation results match surprisingly well to GMPEs, especially considering that this is one realization instead of the average of 30+ realizations of the source. All three methods match the GMPE predictions best at periods shorter than 2.0s, and EXSIM (middle) matches the long periods best out of the three. G&P (top) and EXSIM have narrower standard deviation bands than SDSU (bottom), representing less spread of GMPE Ratio between the 60 stations. With these relationships in mind, we next consider Figure 1a. This column of plots illustrates Sa Ratio versus spectral period for G&P/EXSIM (top), SDSU/EXSIM (middle) and SDSU/G&P (bottom). For EQ3.0 G&P and EXSIM are very similar up to 1.0s period. Then, at longer periods G&P predicts significantly larger Sa. SDSU predicts larger Sa than EXSIM for the entire period range, although this overprediction is relatively small and nearly constant (i.e. almost zero slope in Sa Ratio) for periods less than 1.0s. At longer periods, SDSU acts in the same manner as G&P relative to EXSIM since both methods use the same long period approach. At high frequencies (T<1.0s) for EQ3.0, SDSU predicts larger Sa than G&P. This difference is most pronounced at the shortest periods, up to about 0.05s, where the log ratio is approximately 0.5. Between 0.06s and 1.0s the Sa Ratio is positive but closer to zero, and stays almost constant.

Considering all the simulated scenarios, we make the following general conclusions. The best match between all three methods occurs at shorter periods, specifically at T < 2.0s. The three methods

give more similar results for the Mw 7.0 scenarios than for the Mw 6.6 and Mw 6.2 scenarios. For Mw 6.2 and Mw 6.6 (EQ1.0 - EQ3.0), G&P and SDSU Sa predictions are larger than EXSIM at periods longer than 1.0s, where G&P and SDSU tend to overpredict the GMPEs and EXSIM tends to underpredict. As short periods G&P and EXSIM are more similar than SDSU, and at long periods G&P and SDSU are identical, as expected. Directivity is seen at long periods for both G&P and SDSU, but not for EXSIM. The effect of directivity on Sa is particularly noticeable for EQ4.0 (a Mw 7.0 reverse fault) updip from the hypocenter, and for EQ5.0 (a Mw 7.0 vertical strike slip fault) away from the hypocenter along strike. Different techniques exhibit varying degrees of dependence on rupture propagation direction. G&P has the highest systematic distribution of Sa in space, whereas SDSU contains the highest amount of randomness in space, with EXSIM somewhere in between (i.e. Figure 1c, Figure 1d).

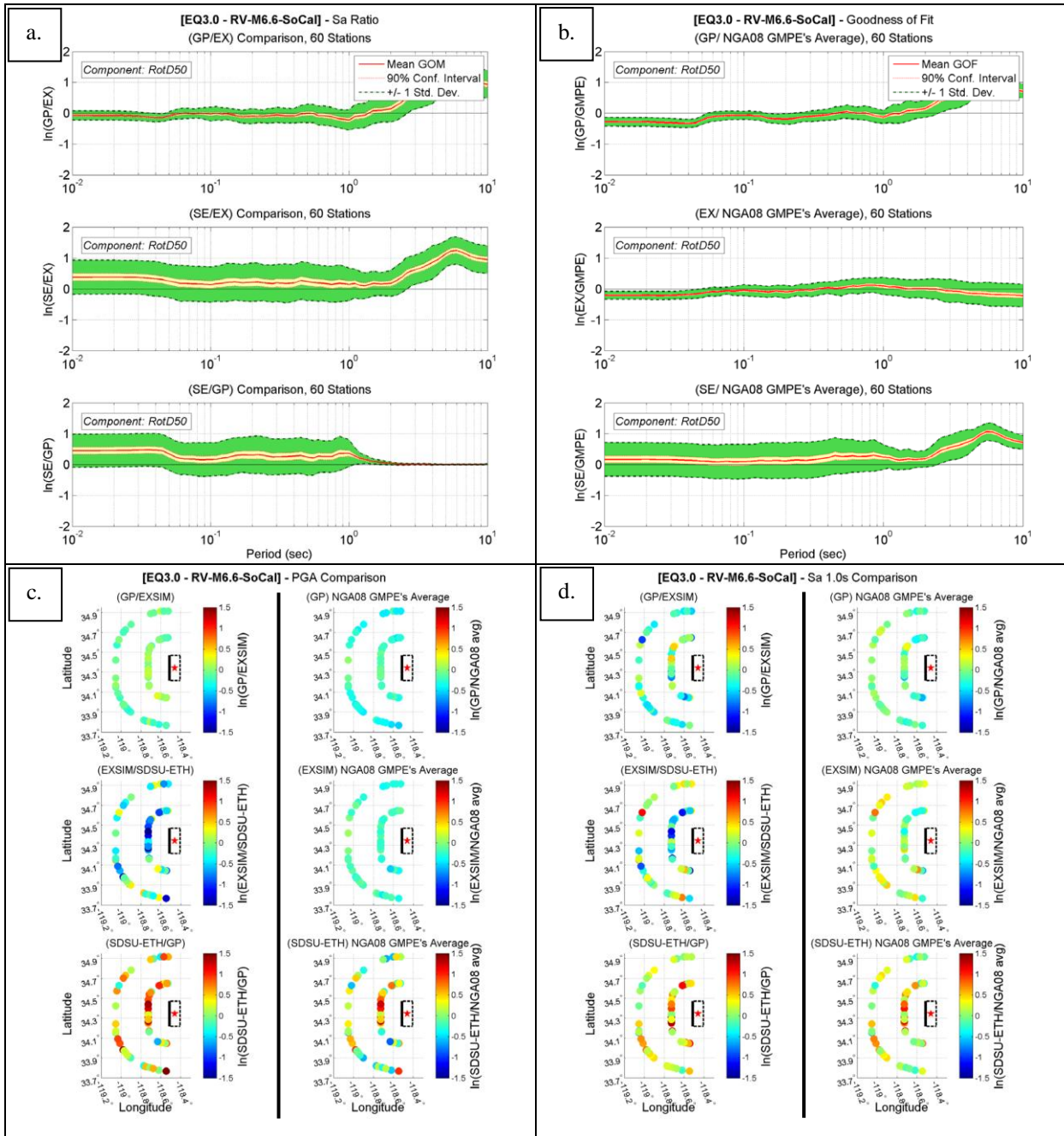


Figure 1. Results for EQ3.0. (a) Sa Ratio versus spectral period ( $T$ ) for G&P/EXSIM (top), SDSU/EXSIM (middle) and SDSU/G&P (bottom). (b) GMPE Ratio versus  $T$  for G&P (top), EXSIM (middle) and SDSU (bottom). (c) Sa Ratio (left column) and GMPE Ratio (right column) maps at PGA. (d) Sa Ratio (left column) and GMPE Ratio (right column) maps at  $T = 1.0$ s.

## REFERENCES

- Atkinson GM, Boore DM, Assatourians K, Campbell K, Motazedian D (2009) "A guide to differences between stochastic point-source and stochastic finite-fault simulations", *Bulletin of the Seismological Society of America* 99, 3192-3201.
- Bayless J, Pitarka A, Ni S, Somerville P (2011) "Validation of broadband strong motion simulations for the NGA East Project – summary of results", [http://peer.berkeley.edu/ngaeast/wp-content/uploads/2011/10/Th\\_AM\\_3\\_Bayless-Somerville\\_URS-Validation-Results.pdf](http://peer.berkeley.edu/ngaeast/wp-content/uploads/2011/10/Th_AM_3_Bayless-Somerville_URS-Validation-Results.pdf)
- Boore DM (2009) "Comparing stochastic point-source and finite-source ground-motion simulations: SMSIM and EXSIM", *Bulletin of the Seismological Society of America* 99, 3202-3216.
- Boore DM (2010) "Orientation-independent, non geometric-mean measures of seismic intensity from two horizontal components of motion", *Bulletin of the Seismological Society of America* 100, 1830-1835.
- Dreger DS, Beroza GC, Day SM, Goulet CA, Jordan TH, Spudich PA, Stewart JP (2013) "Evaluation of SCEC Broadband Platform Phase 1 Ground Motion Simulation Results", *Submitted August 1, 2013*.
- Graves R, Pitarka A (2010) "Broadband ground motion simulation using hybrid approach", *Bulletin of the Seismological Society of America* 100, 5A, 2095-2123.
- Mai PM, Imperatori W, Olsen KB (2010) "Hybrid broadband ground-motion simulations: combining long-period deterministic synthetics with high-frequency multiple S-to-S back-scattering", *Bulletin of the Seismological Society of America* 100, 2124-2142.
- Mena B, Mai PM, Olsen KB, Purvance MD, Brune JN (2010) "Hybrid Broadband Ground-Motion Simulation Using Scattering Green's Functions: Application to Large-Magnitude Events", *Bulletin of the Seismological Society of America* 100, 2143-2162.
- Motazedian D and Atkinson GM (2005) "Stochastic finite-fault modeling based on a dynamic corner frequency", *Bulletin of the Seismological Society of America* 95, 995-1010.